

AlphaPre: Amplitude-Phase Disentanglement Model for Precipitation Nowcasting

Supplementary Material

1. Dataset Details

SEVIR [26] is a curated and annotated dataset that aligns multiple data types, including visible satellite imagery, infrared satellite imagery (mid-level water vapor and clean longwave window), NEXRAD radar mosaics of vertically integrated liquid (VIL), and ground lightning events. The dataset comprises 20,393 weather events captured from 2017 to 2020, each event providing a 4-hour sequence of images sampled every 5 minutes, covering a 384 km × 384 km area across the continental U.S. To predict future VIL frames up to 20 time steps (100 minutes) based on 5 observed frames (25 minutes), we sample 25 consecutive frames with a stride of 13 for each event. The dataset is split into training, validation, and test sets using January 1, 2019, and June 1, 2019, as the cutoff dates. Frames are rescaled to the range 0-255 and binarized at thresholds [16, 74, 133, 160, 181, 219] to compute CSI and HSS.

MeteoNet [15] is a multimodal dataset containing full time series of satellite and radar images, weather models, and ground observations. It covers a 550 km × 550 km area in northwestern France and spans over three years (2016-2018), with recordings every 5 minutes. Similar to SEVIR, we split the radar sequences from 2016 to 2018 into training, validation, and test sets using January 1, 2018, and June 1, 2018, as cutoff dates. The thresholds set to [12, 18, 24, 32] for CSI and HSS evaluation, following [?].

The **Shanghai Radar** [5] dataset consists of continuous radar echo frames generated by volume scans at approximately 6-minute intervals between October 2015 and July 2018 in Pudong, Shanghai. Each radar echo map covers an area of 501 km × 501 km. We preprocess the echo sequences following [?]. The data range for the frames is set to [0-70], and thresholds are set to [20, 30, 35, 40] for computing CSI and HSS.

The **CIKM** [24] dataset comes from the CIKM AnalytiCup 2017 Competition, recording precipitation events within a 101 km × 101 km area in Guangdong, China. Each sample includes 15 historical radar echo maps with a 6-minute interval between consecutive maps. We process the dataset following DiffCast [39], padding each echo map to 128 × 128 pixels and splitting it into training, validation, and test sets as per the original setup. Pixel values in each frame are transformed to reflectivity values ranging from [0, 76] dBZ, and thresholds of [20, 30, 35, 40] are used to compute CSI and HSS. The specific data statistics are provided in Table 1.

Dataset	N_{tr}	N_{va}	N_{te}	(C, H, W)	T_i	T_o
SEVIR	23808	6016	8100	(1,128,128)	5	20
MeteoNet	6308	1310	1310	(1,128,128)	5	20
Shanghai	1534	526	526	(1,128,128)	5	20
CIKM	8000	2000	4000	(1,128,128)	5	10

Table 1. Dataset statistics. N_{tr} , N_{va} and N_{te} denote the number of instances in the training, valid and test sets.

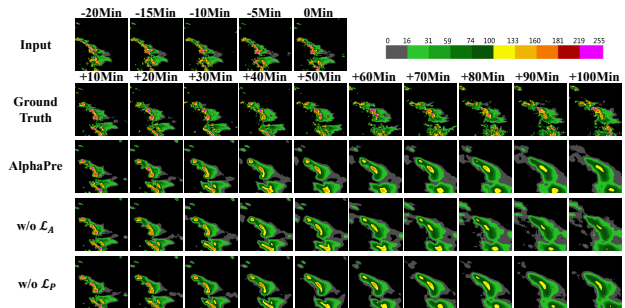


Figure 1. Ablation study visualization on the SEVIR dataset.

2. Additional Ablation Studies

In this section, we provide additional ablation study analyses. Our model incorporates two additional loss functions, and we conducted ablation experiments to analyze their effectiveness. Fig. 1 presents a visualized comparison: w/o \mathcal{L}_A indicates the removal of the amplitude loss, while w/o \mathcal{L}_P represents the removal of the phase loss. As shown, when the amplitude loss is removed, the predicted results exhibit significantly reduced intensity, though many details remain intact. In contrast, when the phase loss is removed, the predictions become smoother, but the intensity remains relatively accurate. This further validates the effectiveness of the two loss functions designed in our model.

3. More Qualitative Results

In this section, we provide additional visualization examples, as shown in Fig. 2, 3, 4 and 5. Compared to other deterministic models, our approach predicts more accurate precipitation intensity and location. Compared to DiffCast, which incorporates a diffusion model, our precipitation contours are less sharp, but the precipitation location is more accurate.

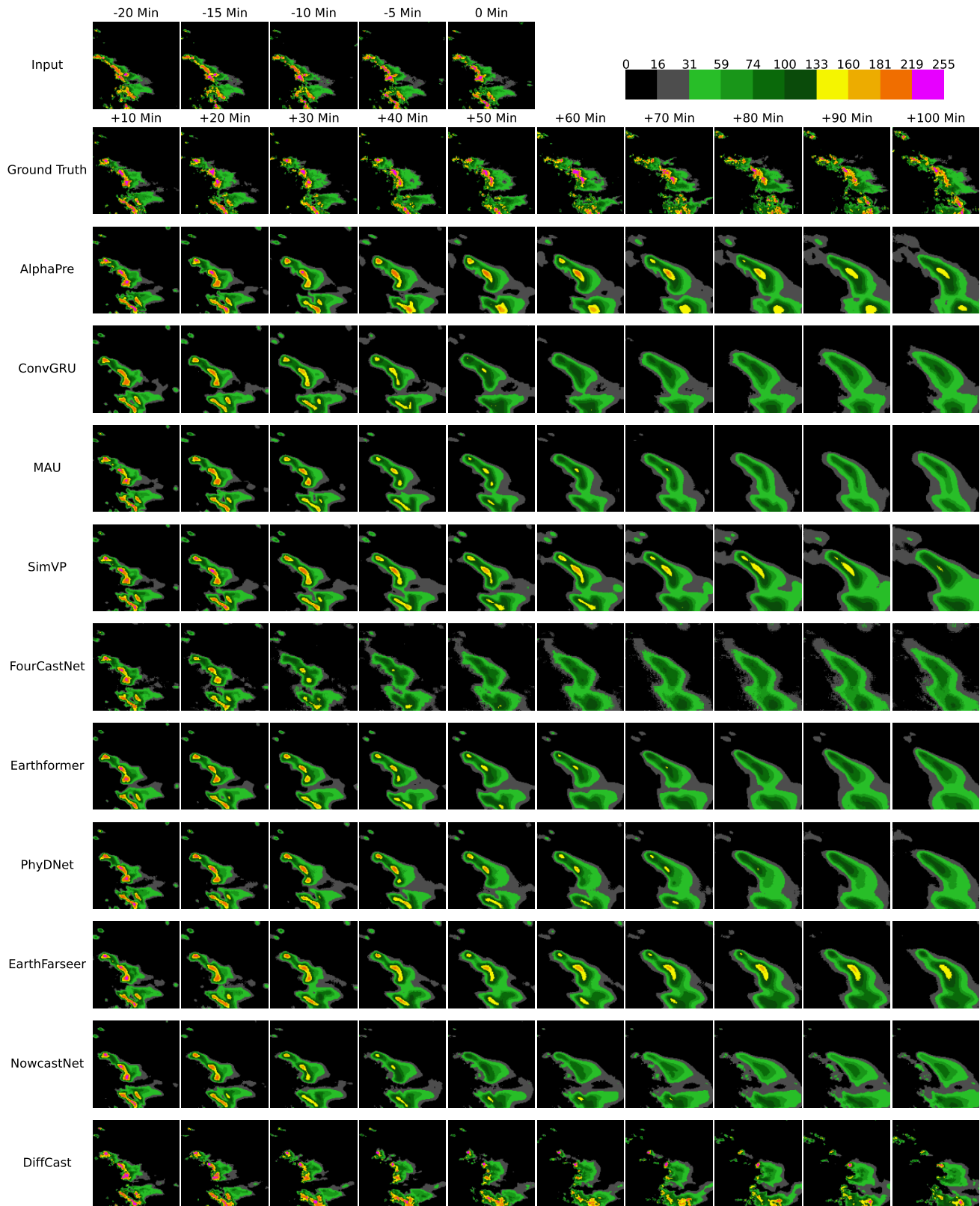


Figure 2. Prediction examples on the SEVIR dataset.

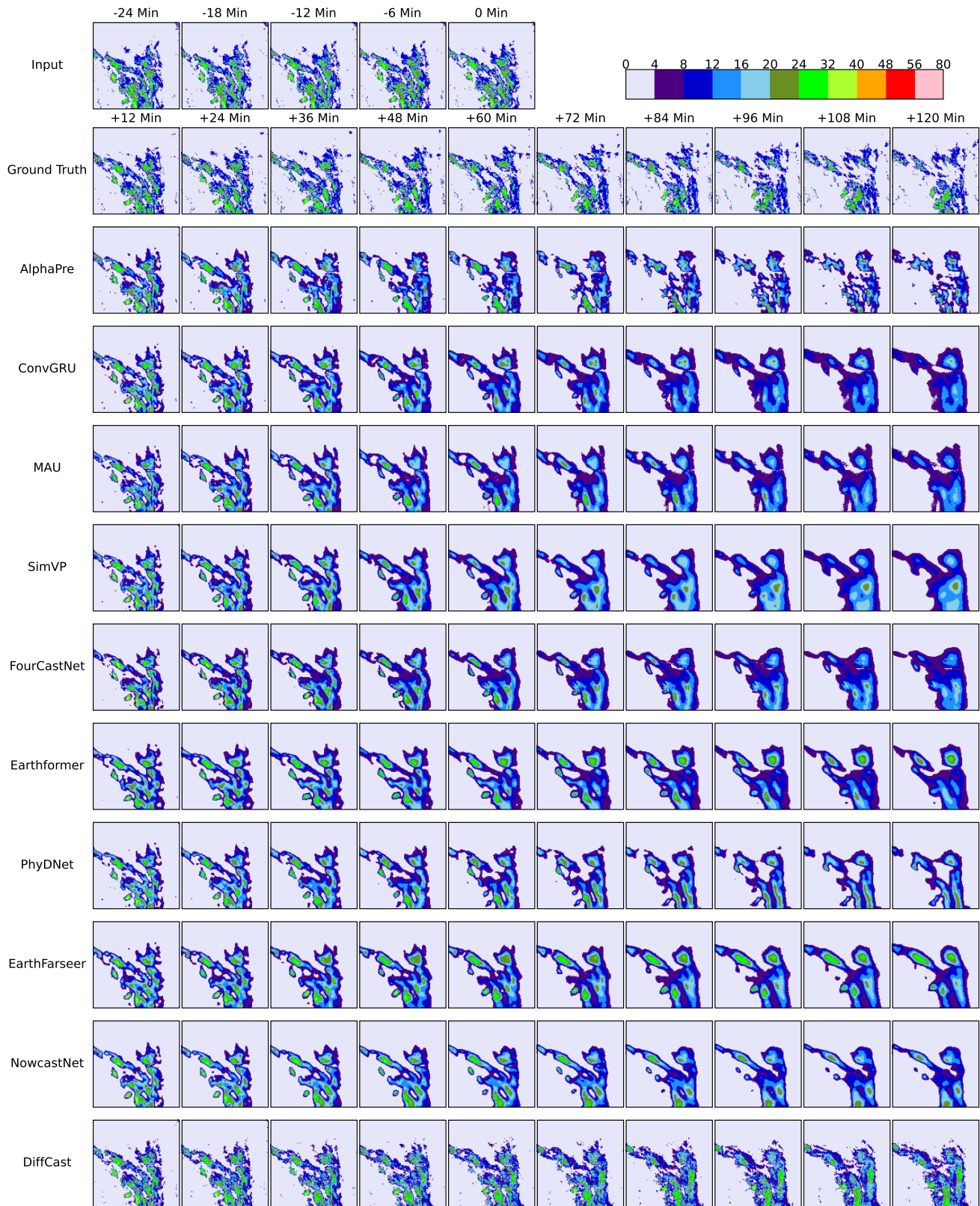


Figure 3. Prediction examples on the MeteoNet dataset.

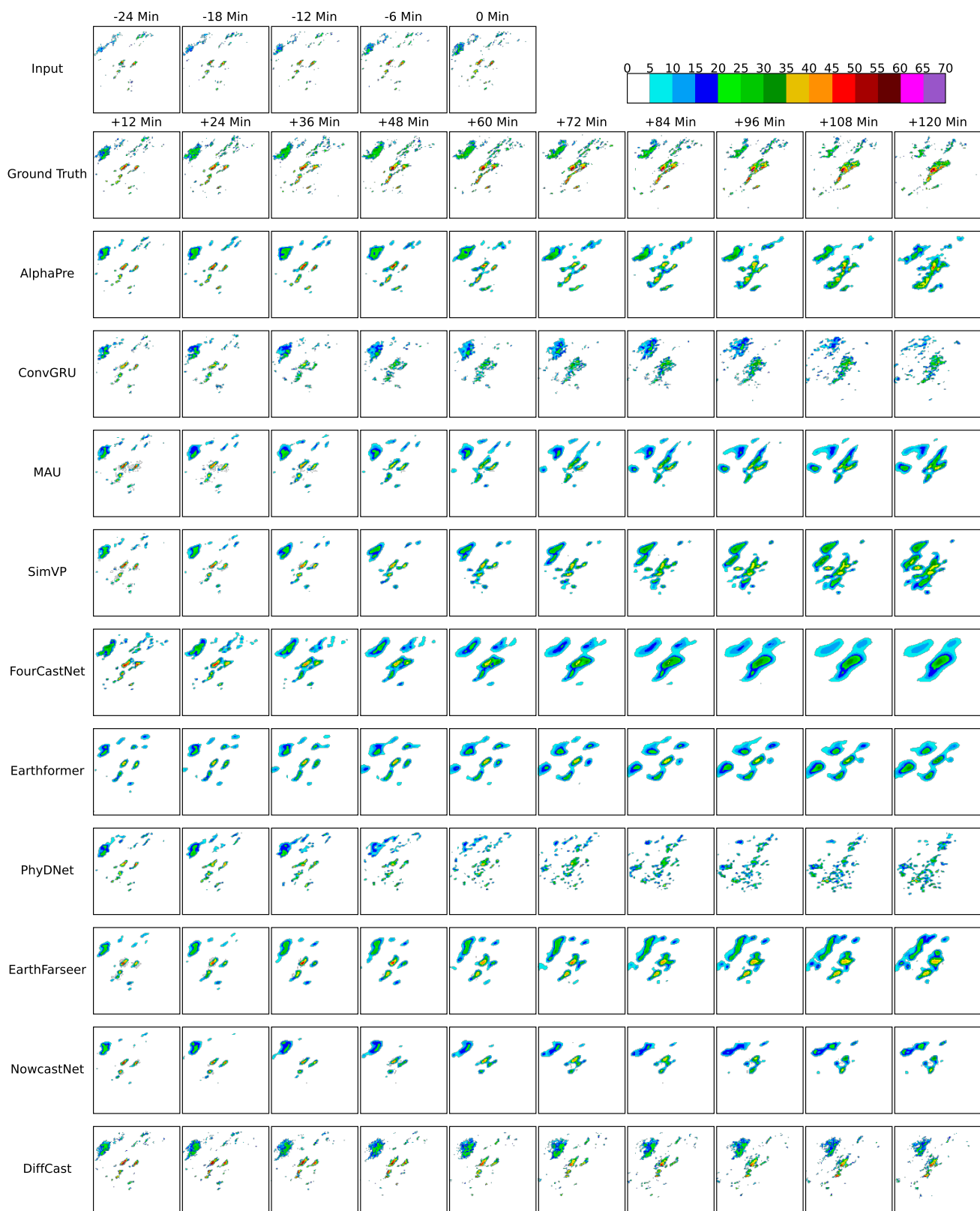


Figure 4. Prediction examples on the shanghai dataset.

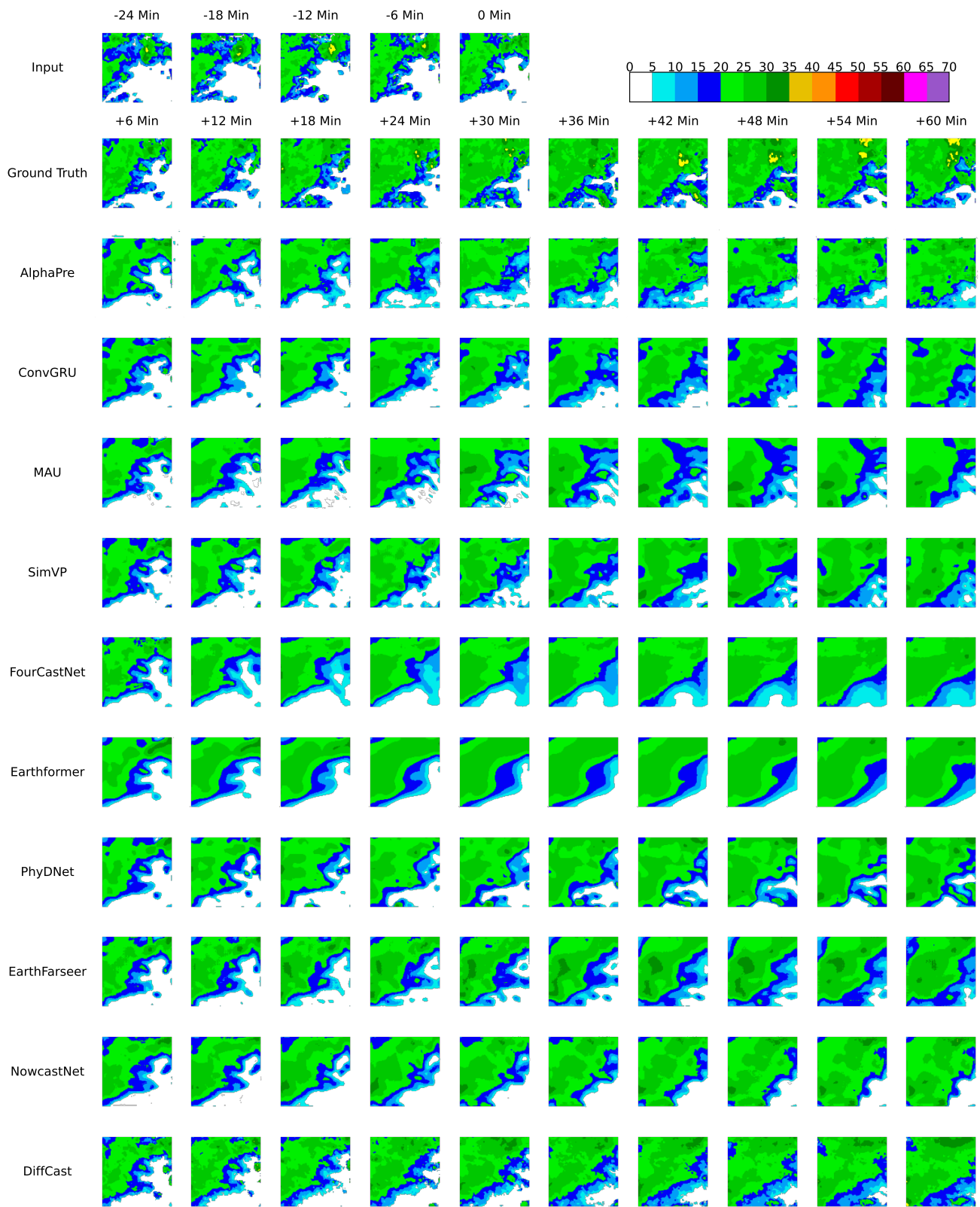


Figure 5. Prediction examples on the CIKM dataset.